Human Molecular Genetics, 2014, Vol. 23, No. 4 **1073–1083**
doi:10.1093/hmg/ddt502
Advance Access published on October 16, 2013

Mutations in *MAP3K1* tilt the balance from SOX9/FGF9 to WNT/β-catenin signaling

Johnny Loke[1], Alexander Pearlman[1], Orietta Radi[3], Orsetta Zuffardi[3], Ursula Giussani[4], Rosanna Pallotta[5], Giovanna Camerino[3] and Harry Ostrer[1,2,*]

[1]Department of Pathology and [2]Department of Genetics and Pediatrics, Albert Einstein College of Medicine, Bronx, NY 10461, USA [3]Medicina Molecolare, Biologia Generale e Genetica Medica, Università di Pavia, Pavia, Italy [4]Department of Medical Genetics, Ospedali Riuniti,Bergamo, Italy [5]Department of Medicine and Aging Sciences, 'G. D'Annunzio' University of Chieti-Pescara, Chieti-Pescara, Italy

Received June 24, 2013; Revised September 25, 2013; Accepted October 3, 2013

In-frame missense and splicing mutations (resulting in a 2 amino acid insertion or a 34 amino acid deletion) dispersed through the *MAP3K1* gene tilt the balance from the male to female sex-determining pathway, resulting in 46,XY disorder of sex development. These *MAP3K1* mutations mediate this balance by enhancing WNT/β-catenin/FOXL2 expression and β-catenin activity and by reducing SOX9/FGF9/FGFR2/SRY expression. These effects are mediated at multiple levels involving *MAP3K1* interaction with protein co-factors and phosphorylation of downstream targets. In transformed B-lymphoblastoid cell lines and NT2/D1 cells transfected with wild-type or mutant *MAP3K1* cDNAs under control of the constitutive CMV promoter, these mutations increased binding of RHOA, MAP3K4, FRAT1 and AXIN1 and increased phosphorylation of p38 and ERK1/2. Overexpressing RHOA or reducing expression of MAP3K4 in NT2/D1 cells produced phenocopies of the *MAP3K1* mutations. Using siRNA knockdown of RHOA or overexpressing MAP3K4 in NT2/D1 cells produced anti-phenocopies. Interestingly, the effects of the *MAP3K1* mutations were rescued by co-transfection with wild-type *MAP3K4*. Although *MAP3K1* is not usually required for testis determination, mutations in this gene can disrupt normal development through the gains of function demonstrated in this study.

INTRODUCTION

Sex determination in mammals is a genetically encoded process that mediates the balance between testis and ovary developmental pathways. To date, much work has focused on the roles of transcription factors (SRY, SOX9, NR0B1), growth factors (FGF9, PDGF) and signaling molecules (WNT4, RSPO1, β-catenin) that regulate these pathways (1–3). Knockout of these genes in the permissive developing gonad or overexpression in the non-permissive developing gonad lead to genetic sex reversal. Examples of these effects include homozygous loss-of-function alleles in RSPO1 and ectopic expression of SRY and SOX9 all leading to 46,XX testicular disorder of sex development as well as knockout of SRY and SOX9 and overexpression of WNT4 and stabilization of β-catenin leading to ovarian development or gonadal dysgenesis (4–11). Despite prior observations that signal transduction molecules in the MAP kinase pathway play a role in mediating the expression of these genes and their products, especially in chondrocyte development, their roles in mediating the balance between SOX9/FGF9 expression for testicular determination and WNT/β-catenin expression for ovarian determination is poorly understood (12–14).

Previously, we showed that missense mutations at well-conserved sites or in-frame splicing variants with in-frame insertion in *MAP3K1* resulted in 46,XY gonadal dysgenesis and milder forms of this phenotype based on co-inheritance in multiple families (15). We have also demonstrated missense mutations in *MAP3K1* in several cases of sporadic 46,XY gonadal dysgenesis. In turn, these mutations altered phosphorylation of the downstream targets, p38 and ERK1/2, and increased binding of the co-factors, RHOA and MAP3K4 as shown in our previous studies (16). Yet, knockout of the *MAP3K1* gene itself led to only minor testicular abnormalities in the developing mouse

*To whom correspondence should be addressed at: Department of Pathology, Albert Einstein College of Medicine, 1300 Morris Park Avenue, Ullman 817, Bronx, NY 10461, USA. Tel: +1 7184308605; Email: harry.ostrer@einstein.yu.edu

gonad, suggesting that it is not necessary for testicular development (17). Our previous studies showed a series of N-terminal mutations through exon 10; here, we extend the repertoire of mutations that cause 46,XY gonadal dysgenesis further downstream to exon 13 and 14, spreading across multiple functional domains of MAP3K1 (15). We observed that these mutations tilt the balance in the sex-determining pathways not only by upregulating β-catenin expression and activity, but also at multiple levels by downregulating SOX9, SRY, FGF9 and FGFR2 expression. The effects of these mutations in *MAP3K1* were rescued by co-transfection with wild-type *MAP3K4* in NT2/D1 cells.

RESULTS

Mutations in *MAP3K1* increase phosphorylation of downstream targets and binding of associated proteins. In the current study, we examined six different mutations in the *MAP3K1* gene, five of which caused abnormal developmental phenotypes (Fig. 1, Table 1). These mutations have the characteristic of being in-frame alterations, either non-conservative single-nucleotide variants (p.P153L, p.L189R, p.L189P, p.K246E) or familial splice acceptor site variant (c.634-8T>A and c.2180-2A>G) (Fig. 1C). Previously, we showed that the c.634-8T>A mutation created a novel splice acceptor site that results in insertion of two amino acids residues in-frame between codons 211 and 212 (15). The c.2180-2A>G mutation results in skipping exon 13 or use of a cryptic acceptor at c.2283_2284; chr5:56177013-5617714 (UCSC hg19) with loss of 34 amino acid residues in-frame between codons 727 and 761 (Fig. 1C). Thus, these mutations occurred in exons 2, 3, 13 and 14 of this 20 exon gene. Transformed B-cell lymphoblastoid cell lines (LCLs) were available for all of these mutations. These were used for analysis of phosphorylation of downstream targets, interactions with MAP3K1-binding proteins, or relative abundance of β-catenin.

As we have reported previously for the p.L189P, p.L189R and c.634-8A mutations that were associated with gonadal dysgenesis, analysis of the LCLs for the newly identified mutations demonstrated varying increases in phosphorylation of the downstream targets, p38 and ERK1/2, and increases in binding of

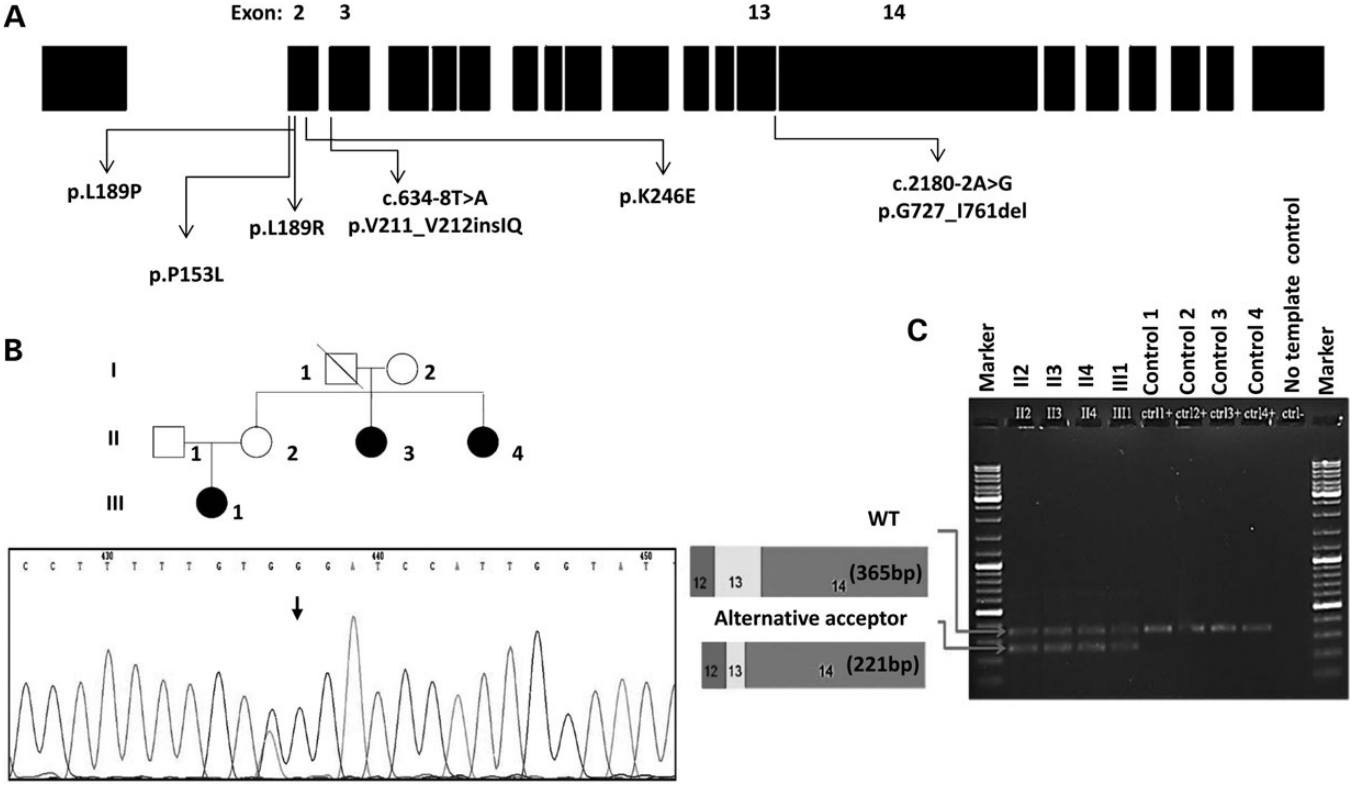

Figure 1. (**A**) *MAP3K1* mutations reported in this study include missense (p.P153L, p.L189R, p.L189P, p.K246E) and splicing (c.634-8T>A and c.2180-2A>G). The c.634-8T>A mutation creates a novel splice acceptor site that results in the insertion of two amino acids residues in-frame between codons 211 and 212 (15). The c.2180-2A>G mutation results in use of a cryptic acceptor at c.2283_2284; chr5:56177013-5617714 (UCSC hg19) with loss of 34 amino acid residues in-frame between codons 727 and 761. (**B**) Pedigree of multiple individuals with biopsy-proven 46,XY gonadal dysgenesis and MAP3K1 c.2180-2A>G mutation (II-3, II-4 and III-1). All three individuals with 46,XY mutations had an unvirilized female phenotype and dysgenetic gonads at histology. The uterus of Subject II-3 was observed at laparoscopy and Subjects II-3 and II-4 had elevated LH and FSH. Individual II-2 was an unaffected 46,XX carrier. Sanger sequencing demonstrated the heterozygous splicing site mutation in Subject II-3. (**C**) The mutation was predicted to affect splicing in one of three ways: (1) skipping of exon 13 (causing a frameshift insertion of a STOP codon after seven amino acids, resulting in complete loss of the kinase domain (c.2180_2369del; p.Ser728Ilefs*8), (2) use of a cryptic acceptor site within exon 13 (c.2283_2284 AG;g.56177013-5617714AG). In this case, the mutated mRNA would lose the first 105 nucleotides of exon 13 (c.2180_2284del), preserving the open reading frame and resulting in a protein with the first 35 amino acids of exon 13 deleted (p.Gly727_Ile761del), or (3) a normal transcript. RT–PCR with primers external to the exons involved in the mutations results in two bands corresponding by size to the wild type and to the form that uses the cryptic acceptor splice site internal to exon 13. Cloning of the RT–PCR product and sequencing of colonies showed the presence of both variant splicing forms (using the cryptic acceptor site internal to exon 13 and exon 13 skipping) along with the wild-type form.

Table 1. Binding threshold depicted in mean ± SD for six MAP3K1 mutants LCLs and their phenotypic effects

Mutation	Type	Gonadal dysgenesis	P38 phosphorylation	ERK1/2 phosphorylation	RHOA binding	MAP3K4 binding	SOX9 mRNA	β-Catenin mRNA	β-Catenin activity
p.P153L	Missense	Yes	3.90.0291	5.2 ± 0.0356	40 ± 0.0590	5.0 ± 0.0258	NA	NA	NA
p.L189R	Missense	Yes	1.9 ± 0.0422	2.6 ± 0.0511	2.1 ± 0.0407	3.0 ± 0.0491	−7.0 ± 0.0542	3.8 ± 0.1050	3.0 ± 0.1533
p.L189P	Missense	Yes	2.1 ± 0.0218	2.5 ± 0.0398	2.8 ± 0.0592	3.2 ± 0.0703	−6.3 ± 0.0658	6.4 ± 0.0746	3.6 ± 0.3174
p.K246E	Missense	No	1.3 ± 0.0398	No change	No change	2.0 ± 0.0512	NA	NA	NA
c.634-8T>A	In-frame splicing p.V211_V212insIQ	Yes	2.3 ± 0.0652	3.3 ± 0.0708	2.5 ± 0.0398	2.8 ± 0.0238	−4.7 ± 0.0445	13.7 ± 0.0137	7.5 ± 0.2596
c.2180-2A>G	In-frame splicing p.G727_I761del	Yes	4.6 ± 0.0299	6.2 ± 0.0463	28 ± 0.0212	15 ± 0.0452	NA	NA	NA

RHOA and MAP3K4 (Fig. 2A–C, Supplementary Material, Fig. 1S, Table 1) (15,16). The phosphorylation of ERK1/2 and the binding of RHOA were measured by immunoprecipitation western blot analysis and confirmed by the flow-variant analysis (FVA) method that uses modified immunoprecipitation with flow cytometry to measure the binding of specific proteins to fluorochrome-coupled antibodies (16). The p38 phosphorylation and RHOA binding in the non-pathogenic hypomorphic p.K246E variant LCL were only slightly increased compared with the wild-type male LCL control and significantly less than in the other mutation-bearing LCLs. We have examined a total of 11 wild types: seven normal males and four normal females in triplicates of three biological repeats to establish the normal baseline control. The phosphorylation of ERK1/2 and the binding of MAP3K4 to MAP3K1 in the p.K246E-bearing LCL were not increased compared with the control.

This increased binding was not confined to RHOA and MAP3K4, previously MAP3K1 has been shown to bind AXIN1 in various truncated deletion models, which in turn, binds to FRAT1 (18–20). FVA performed on wild-type or mutant LCLs using MAP3K1 as bait showed increased binding to FRAT1 and AXIN1 for those bearing the p.L189P and p.153L mutations, but not the p.K246E variant. The increased binding of AXIN1 to MAP3K1 is independent of the binding of FRAT1 to MAP3K1 (Fig. 2D).

The effects of MAP3K1 mutations on phosphorylation of downstream targets and binding of associated proteins can be recapitulated in NT2/D1 cells. Human teratocarcinoma cell line NT2/D1 has been shown previously to express the repertoire of genes observed in testis determination and has been used to examine the effects of mutations in SF1 and upregulation of β-catenin on the expression of SOX9 (21,22). Transfection of mutant and wild-type cDNAs with CMV-driven expression plasmids led to efficient expression of MAP3K1 (Supplementary Material, Fig. S2A). The p.L189P, p.L189R and c.634-8A mutations increased phosphorylation of p38 and ERK1/2, as had been observed in LCLs previously (15). These increases in phosphorylation were detected using standard western blots (Fig. 3A, Supplementary Material, Fig. 1S) and phosphorylated digital cell western (DCW) where expression of multiple target proteins (total and phosphorylated) are measured in large numbers of intact fixed cells simultaneously (Fig. 3B). Using the co-immunoprecipitation method of FVA, the NT2/D1 cells transfected with the p.L189P, p.L189R and c.634-8A mutant cDNAs showed increased RHOA binding to MAP3K1 bait on the epoxy-coated beads (*Y*-axis) and forward scatter (FSC-A—*X*-axis), as has been observed previously in LCLs (Fig. 3C) (15). FSC is the light scatter fluorescence measured at low-angle forward proportional to the diameter of the bead or cell. FSC provides a suitable method for detecting particles greater than a given size, independent of their fluorescence. Although overexpression of the wild-type *MAP3K1* cDNA increased both RHOA binding and p38 and ERK1/2 phosphorylation, these effects were ∼2.5-fold increased when the mutant cDNAs were transfected (Fig. 3D).

Mutations in MAP3K1 tilt the balance of gene expression in the testis-determining pathway. Three mutations, p.L189P, p.L189R and c.634-8A, were studied in greater detail to understand their effects on the testis-determining pathway. Transfection of these mutant cDNAs decreased expression of SOX9

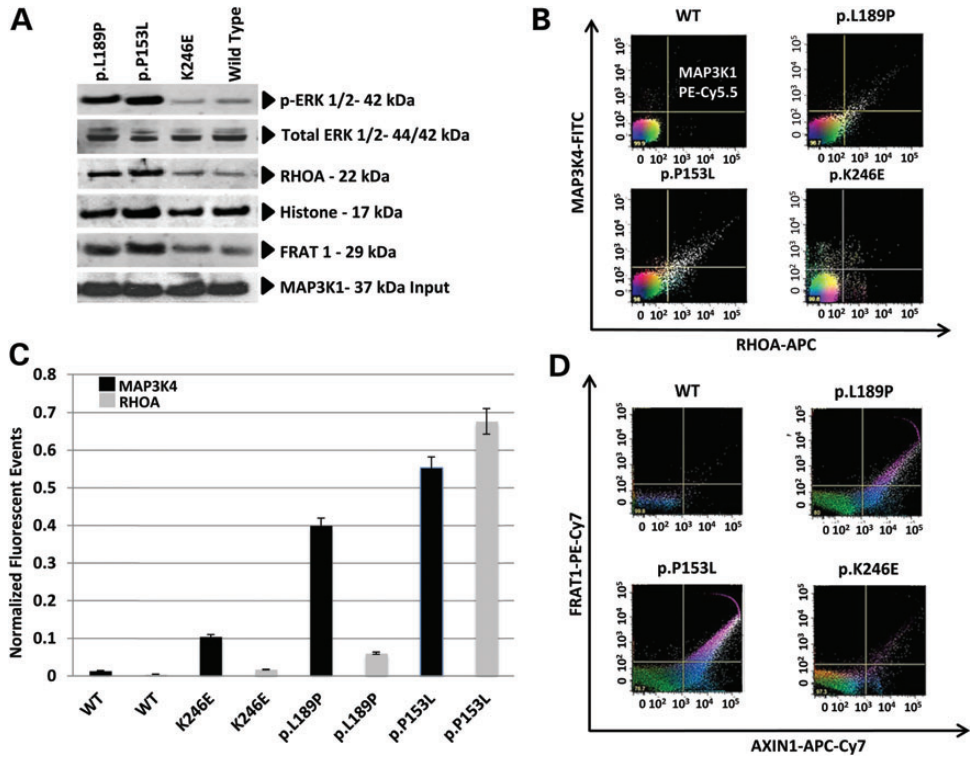

Figure 2. Mutations in *MAP3K1* increase RHOA, MAP3K4, FRAT1 and AXIN1 affinity to MAP3K1 and phosphorylation of ERK1/2 protein. Two *MAP3K1* mutations (p.L189P and p.P153L) alter the binding of RHOA, MAP3K4, FRAT1, and AXIN1 and phosphorylation of ERK1/2 in mutant LCLs, whereas the p.K246E variant affects only MAP3K4 binding. (**A**) Standard western blot analysis using primary LCLs bearing p.L189P, p.P153L *MAP3K1* mutations showed increased phosphorylation of ERK1/2 protein. Co-immunoprecipitation of these lysates, where *MAP3K1* was the bait, showed increased affinity to RHOA and FRAT1 (probe antibodies). The p.K246E variant did not have an effect that varied from wild-type LCLs. Histone as loading control, and MAP3K1 as input control. (**B**) FVA using primary wild-type LCLs or those bearing p.L189P and p.153L mutations or p.K246E variant was performed using MAP3K1 as bait and showed increased binding to RHOA (*Y*-axis, and as shown in A) and MAP3K4 (*X*-axis). Pseudo primary colors were assigned using FLOWJO 6.0 for each target, MAP3K4—green, RHOA—red and MAP3K1—blue. If all three targets are present on the target bead in equal ratio, a white pixel is generated against the black background. (**C**) Quantification of FVA fluorescence intensity for MAP3K4 (solid black bar) and RHOA (gray bar) binding to MAP3K1 and normalized to MAP3K1 input fluorescence (*Y*-axis is normalized fluorescent events) and compared in a pairwise fashion by Student's *t*-test shown as $^{*}P < 0.05$ and $^{**}P < 0.005$. The binding of MAP3K4 and RHOA was increased for all three variants/mutations, yet significantly higher for the p.L189P and p.P153L mutations. (**D**) FVA using primary wild-type or mutant LCLs was performed using MAP3K1 as bait and showed increased binding to FRAT1 (*Y*-axis, and as shown in A) and AXIN1 (*X*-axis) for those bearing the p.L189P and p.153L mutations, but not the p.K246E variant. Pseudo primary colors were assigned using FLOWJO 6.0 for each target, FRAT1—green, AXIN1—red and MAP3K1—blue. If all three targets are present on the target bead in equal ratio, a white pixel is generated against the black background. If only AXIN1 and MAP3K1 are present on the target bead a pink pixel is generated.

mRNA dramatically, but increased expression of β-catenin mRNA by 30.2-fold for L189P, 8.5-fold for L189R and 97.1-fold for c.634-8A (Fig. 4A and C). The altered expression of SOX9 and β-catenin was also observed at the protein level. SOX9 protein expression compared with wild type was reduced 5.1-fold for L189P, 5.7-fold for L189R and 4.1-fold for c.634-8A (Fig. 4B). At the same time, β-catenin protein expression was increased 11.6-, 5.5- and 27.1-fold, respectively, when NT2/D1 was transfected with the mutant cDNAs, L189P, L189R and c.634-8A (Fig. 4D). To test whether the increased β-catenin expression resulted in increased β-catenin activity, co-transfection experiments were performed with the TCF/LEF Cignal dual-luciferase reporter expression vector system to measure WNT signal transduction using the luciferase reporter cDNA under the control of the β-catenin-inducible LEF1 promoter. As expected, co-transfection of the p.L189P, p.L189R and c.634-8A mutant cDNAs significantly increased TCF/LEF1 luciferase activity (Fig. 5A). We also examined FGF9, FGFR2 and FOXL2 mRNA expression in NT2/D1 cells transfected with the mutant or wild-type cDNAs. Transfection of these mutant cDNAs resulted in a marked reduction of expression for FGF9 (Fig. 5B) and FGFR2 (Fig. 5C). We observed increased FOXL2 mRNA expression in the mutant transfections—3.5-fold for L189P, 2.5-fold for L189R and 10.6-fold for c.634-8A (Fig. 5D). The increased FOXL2 mRNA expression demonstrated that the increased β-catenin was biologically active.

Modulating the expression of the MAP3K1-binding partners produced molecular phenocopies of MAP3K1 mutations, RHOA and MAP3K4. The expression of RHOA and MAP3K4 were modulated by transfection of wild-type cDNAs for the respective genes or by knockdown using specifically targeted Stealth-siRNAs. The Stealth-siRNAs did not cause off-target effects (Supplementary Material, Fig. S2C). These genes had mutually antagonistic effects on the downstream signaling pathways for SOX9 and β-catenin as well. Overexpression of RHOA and knockdown of MAP3K4 led to diminished expression of SOX9 and enhanced mRNA expression of β-catenin by 81.5- and

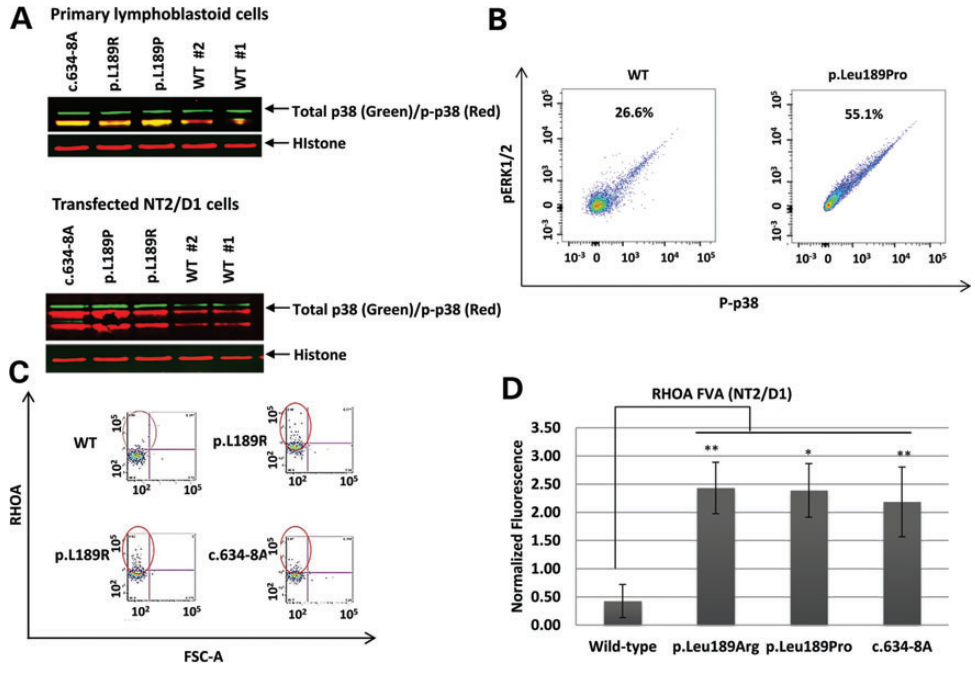

Figure 3. Transfected NT2/D1 cells using with expression plasmids bearing wild-type or mutant *MAP3K1* cDNAs shows similar increased phosphorylation of p38 protein. Mutations in *MAP3K1* increase RHOA affinity to MAP3K1 when transfected with any of the three mutant *MAP3K1* (p.L189R, p.L189P and c.634-8A) cDNAs. (**A**) Standard western blot analysis using primary LCLs and transfected NT2/D1 cells bearing p.L189P, p.L189R and c.634-8A mutations showed increased phosphorylation of p38, histone as loading control. (**B**) Transfected NT2/D1 cells analyzed by modified flow cytometry to detect phosphorylated protein abundance analysis (DCW: see Materials and Methods) demonstrated increased phosphorylation of p38 in p.L189P mutation-bearing versus wild-type cells (55.1 versus 26.6 normalized fluorescent unit of phospho-p38, respectively). (**C**) FVA performed on NT2/D1 cells transfected with expression plasmids bearing wild-type or mutant (p.L189R, p.L189P, and c.634-8A) *MAP3K1* cDNAs, followed by overnight flow-based immunoprecipitation using MAP3K1 as bait and showed increased binding to RHOA (*Y*-axis) normalized to MAP3K1 input fluorescence, compared with forward scatter (FSC-A) (*X*-axis). (**D**) FVA quantification of RHOA binding to MAP3K1 normalized to MAP3K1 (*Y*-axis is normalized fluorescent events) and compared in a pairwise fashion by Student's *t*-test, $^{*}P < 0.05$ and $^{**}P < 0.001$. The binding of RHOA to MAP3K1 in NT2/D1 cells was increased for mutant transfected compared with wild-type transfected cells.

60.5-fold, respectively (Fig. 6A and B), whereas knockdown of RHOA by siRNA and overexpression of MAP3K4 led to the opposite effects—increased expression of SOX9 levels by 508- and 171-fold, respectively, and dramatically decreased expression of β-catenin levels (Fig. 6A and B). Thus, overexpression of RHOA and knockdown of MAP3K4 provided phenocopies of the *MAP3K1* mutations in the MAP kinase signaling pathway, suggesting that overexpression of wild-type MAP3K4 could rescue the effects of *MAP3K1* mutations.

The effects of MAP3K1 mutations were rescued by co-transfection with wild-type MAP3K4. To test for *MAP3K4* rescue of *MAP3K1* mutations, co-transfection experiments were performed using a wild-type *MAP3K4* plasmid and wild type or mutant *MAP3K1* plasmids efficient transfection into NT2/D1 cells (Supplementary Material, Fig. S2B). In separate experiments, the NT2/D1 cells transfected with only mutant *MAP3K1* cDNAs (p.L189P, p.L189R and c.634-8A) were compared with cotransfected mutant cDNAs with *MAP3K4* showed restoration of the mRNA and protein expression of SOX9 in mutants (Fig. 4A and B) and, for β-catenin levels, MAP3K4 restored the mutants to wild-type levels (Fig. 4C and D), that is, the expression of SOX9 was increased and the expression of β-catenin was reduced in mutants when MAP3K4 was introduced by transfection. Moreover, the reduction in β-catenin expression was confirmed by TCF dual-luciferase reporter showing similar reduction in β-catenin activity in mutant cotransfected with MAP3K4 (Fig. 5D). Thus, *MAP3K4* rescued the effects of *MAP3K1* mutations. This rescue of the MAP3K1 mutations and of the RHOA overexpression phenocopy appeared to be mediated by increasing SRY expression. Similarly, Taqman qPCR on SRY mRNA expression levels showed marked reduction compared to wild type when the NT2/D1 cells were transfected with mutant MAP3K1 cDNAs or RHOA CMV-driven expression plasmids. Co-transfection with a MAP3K4 expression construct, rescued the SRY mRNA expression in these mutant transfected cells by restoring SRY to that of wild-type cells (Fig. 6C).

DISCUSSION

The development of the embryonic bipotential gonad is genetically controlled. The somatic cell progenitors express both testicular (SOX9/FGF9) and ovarian (WNT4/ β-catenin) factors in a controlled spatial pattern. If SRY is expressed, SOX9 and FGF9 are upregulated via a mutual feedforward loop and the somatic cells adopt a Sertoli fate (1). In turn, SOX9 employs two distinct mechanisms to inhibit WNT/β-catenin signaling. The N-terminus of SOX9 promotes β-catenin degradation, whereas the C-terminus inhibits β-catenin transcriptional activity without affecting its stability (23). Thus, the normal role of *SRY* in XY gonads is to tip the balance toward the testis-specific pathway (4, 6). This pathway can be disrupted by mutations in *SRY*, *SOX9* and SF1, all transcription factors that bind to the

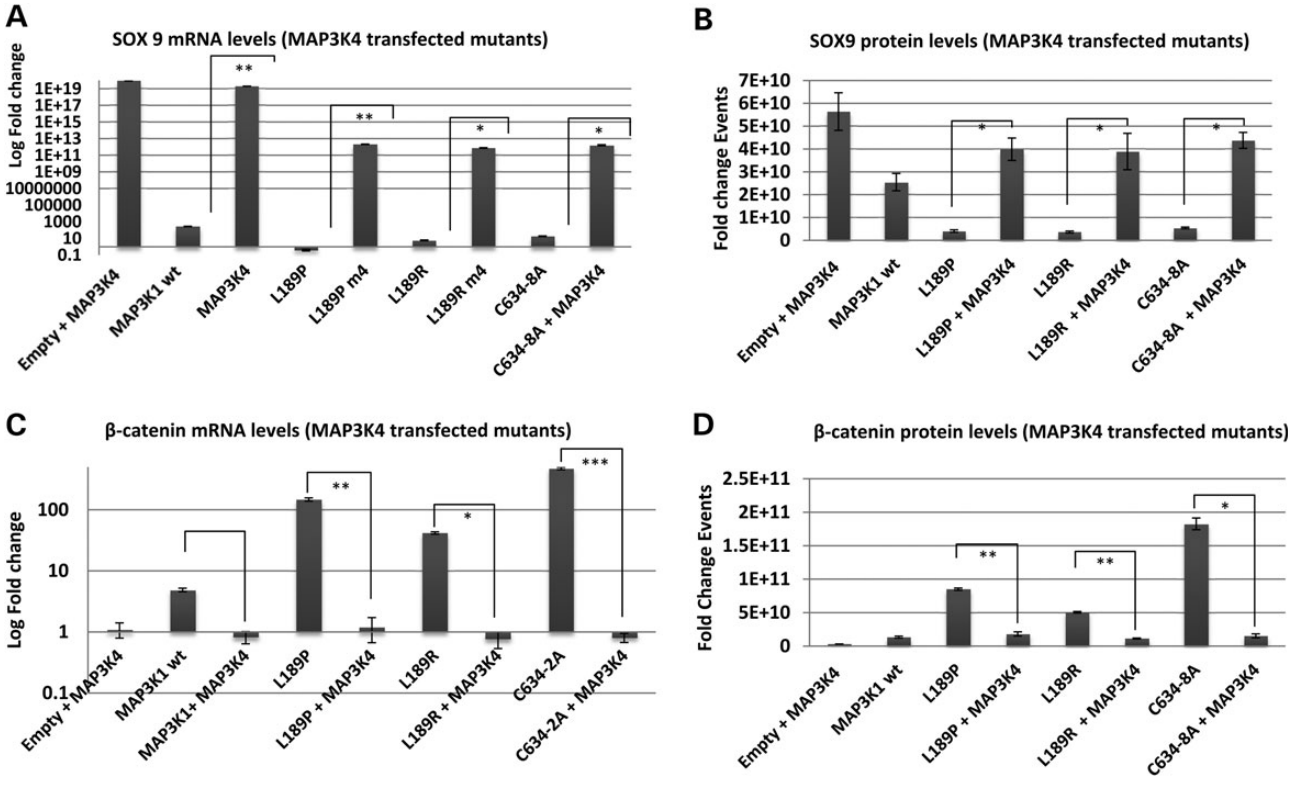

Figure 4. Mutations in *MAP3K1* decrease SOX9 mRNA transcripts and protein and increase β-catenin mRNA transcripts and protein in transfected NT2/D1 cells. Mutant transfected NT2/D1 cells can be rescued by cotransfection with *MAP3K4 cDNA*. qPCR and DCW analyses of mRNA and protein, respectively, at 24 h of NT2/D1 cells transfected with expression plasmids bearing wild-type or mutant (p.L189R, p.L189P, and c.634-8A) cDNAs with or without co-transfection with *MAP3K4*. For Taqman qPCR, results were normalized to housekeeping gene, GAPDH, and compared with control NT2/D1 cells transfected with empty plasmids by Student's *t*-test, $^{*}P < 0.05$ and $^{**}P < 0.005$. (**A**) Quantification of normalized SOX9 mRNA expression by Taqman qPCR (*Y*-axis is fold change relative to empty plasmids) and compared in a pairwise fashion. The mRNA expression of SOX9 was decreased for all three mutations and was rescued by co-transfection with wild-type *MAP3K4* ($P = 0.0002$ for the mutant group versus wild type). (**B**) Quantification of normalized SOX9 protein expression (*Y*-axis is fold change relative to empty plasmids) and compared in a pairwise fashion. The protein expression of SOX9 was decreased when either three mutations were transfected and was rescued by co-transfection with wild-type *MAP3K4* ($P = 0.0003$ for the mutant group versus wild type). (**C**) Quantification of normalized β-catenin mRNA expression (*Y*-axis is fold change relative to empty plasmids) and compared in a pairwise fashion. The mRNA expression of β-catenin was increased for all three mutations and was rescued by co-transfection with wild-type *MAP3K4* ($P = 1.9 \times 10^{-16}$ for the mutant group versus wild type). (**D**) Quantification of normalized β-catenin protein expression (*Y*-axis is fold change relative to empty plasmids) and compared in a pairwise fashion. The protein expression of β-catenin was increased for all three mutant transfected and was rescued by co-transfection with wild-type *MAP3K4* ($P = 0.005$ for the mutant group versus wild type).

SOX9 TESCO enhancer (24). In mice, the pathway can be overridden by a dominant stabilizing mutation in β-catenin (11). Here, we show that the pathway can also be overridden by a series of five different in-frame mutations in *MAP3K1* that were identified in individuals with abnormal gonadal development or by RHOA and MAP3K4 modulations. The effect of these mutations was observed to decrease SOX9 expression and increase β-catenin expression and activity through multiple effects in the MAP kinase pathway (Fig. 7).

The mutations spanned exons 2, 3, 13 and 14 and affected both coding (missense) and splicing. The splicing mutations resulted in insertion of 2 amino acids or deletion of 34 amino acids. Yet, all of the mutations resulting in gonadal dysgenesis caused increased phosphorylation of ERK1/2 and p38 and increased binding of RHOA and MAP3K4 and the representative mutations studied increased binding of AXIN1 and FRAT1 proteins. Therefore, these were a range of sites N-terminal to the MAP3K1 kinase domain that could influence binding of cofactors and increase kinase activity. The increased phosphorylation of ERK1/2 and p38 is known to mediate both inactivation of GSK3β, which, in turn, leads to stabilization, and upregulation of β-catenin (25–27). AXIN1 and FRAT1 also mediate inactivation of GSK3β, AXIN1 interacts with GSK3β to reduce β-catenin abundance, whereas FRAT1 inhibits this process (18–20). Indeed, previous work in β-catenin signaling demonstrated that transfection of siRNA to GSK3β increased expression and activity of β-catenin, similar to our observation of NT2/D1 cell phenocopies of the *MAP3K1* mutations. A previous study showed that AXIN1 association to the MAP3K1 N-terminal region of 'KGANLLIDSTGORL' acted as an activation complex. Upon MAP3K1 depletion in the HEK293T cotransfected with TCF reporter constructs, there was a reduction in TOPFlash activity, suggesting that MAP3K1 is an integral part of AXIN1 sequestration (18). It is possible that FRAT1 and AXIN1 association with MAP3K1 is acting as a sink to promote β-catenin stabilization, but such an observation warrants an independent investigation into the WNT signaling cascade mechanisms.

All of the mutations enhanced binding to RHOA, a known positive regulator of MAP3K1 kinase activity (28). In chondrocytes

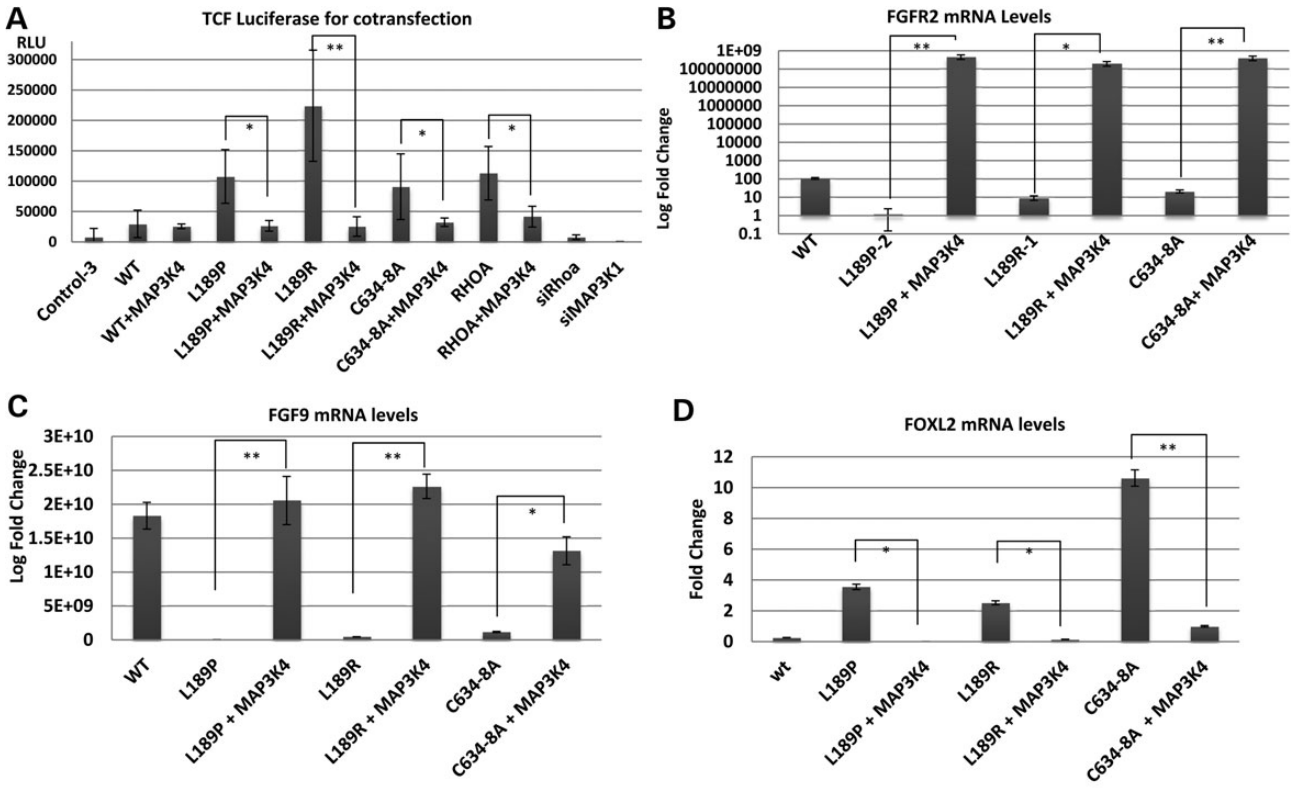

Figure 5. Overexpression of mutant *MAP3K1* increases FOXL2 and decreases FGF9 and FGFR2 mRNA levels and increases of TCF dual-luciferase reporter activity relative to wild type. qPCR analysis of mRNA at 24 h of NT2/D1 cells transfected with expression plasmids bearing wild-type or either mutants (p.L189R, p.L189P, and c.634-8A) cDNAs, a rescue co-transfection is performed alongside with *MAP3K4* for each mutant. Taqman qPCR results were normalized to housekeeping gene, GAPDH, and compared with control NT2/D1 cells transfected with empty plasmids by Student's *t*-test, $^{*}P < 0.05$ and $^{**}P < 0.005$. (**A**) Quantification of normalized TCF/LEF dual reporter luciferase activity (*Y*-axis is normalized relative luciferase units) and compared in a pairwise fashion (mutant versus rescued mutant). Control-3 is the triplicate pool of untreated NT2/D1 cells. The luciferase reporter activity assayed at 48 h following transfection showed marked increase in all three mutants. Overexpression of RHOA similarly increased reporter activity. Knockdown of RHOA or MAP3K1 by either siRNAs abrogated the reporter activity. In separate experiments, co-transfection of any of the three mutants with MAP3K4 rescued their phenotypes, observed as marked reduction of the reporter activity found in mutants. Co-transfection of TCF luciferase reporter with Stealth siRNA to RHOA or MAP3K1 abrogated the reporter activities. (**B**) Quantification of normalized FGFR2 expression (*Y*-axis is fold change relative to empty plasmids) and compared in a pairwise fashion. The expression of FGFR2 was decreased for all three mutations and FGFR2 expression was rescued by co-transfection with wild-type *MAP3K4* into mutants. (**C**) Quantification of normalized FGF9 expression (*Y*-axis is fold change relative to empty plasmids) and compared in a pairwise fashion. The expression of FGF9 was dramatically decreased when NT2/D1 cells were transfected with any of the three mutants. FGF9 expression levels were restored in all mutants' transfected cells when *MAP3K4* was added in separate co-transfection experiments. (**D**) Quantification of normalized FOXL2 mRNA expression (*Y*-axis is fold change relative to empty plasmids) and compared in a pairwise fashion. The expression of FOXL2 was increased for all three mutant transfected NT2/D1 cells, with the highest marked increase observed in C634-8A mutant. MAP3K4 was cotransfected with each mutant in separate experiments showing phenotype rescue similar to wild type.

development, RHOA regulates the transcriptional activity of *SOX9* and its feedback loop (14,29,30). Likewise, we generated phenocopies of the *MAP3K1* mutants by overexpressing RHOA or anti-phenocopies by downregulating expression of RHOA by siRNA transfection. Furthermore, all of the mutations examined here enhanced binding of MAP3K4 to MAP3K1 protein complex. This might have arisen through interactions with their shared binding partner, AXIN1 (31,32). Both MAP kinases compete for AXIN binding, albeit at different sites (31). We have suggested previously that the presence of these *MAP3K1* mutations may alleviate this competition (16). Unlike *MAP3K1*, *MAP3K4* is an essential testis-determining gene. In mice, homozygous loss-of-function alleles in *MAP3K4* lead to disrupted testis development from failure to support cord development (33). This failure of testicular development results from failure to upregulate Sry, an effect mediated by the Map3k4 binding partner, Gadd45γ. In the current experiments, knocking down the expression of MAP3K4-produced molecular phenocopies of the MAP3K1 mutations and overexpressing MAP3K4-produced anti-phenocopies. This overexpression of MAP3K4 corrected the expression patterns of SOX9 and β-catenin and normalized β-catenin activity in co-transfection experiments with *MAP3K1* mutations.

Although bone abnormalities have not been reported in individuals harboring *MAP3K1* mutations, these may nonetheless be present and may represent an ascertainment bias. Heterozygous mutations in the *SOX9* gene with resulting haploinsufficiency cause campomelic dysplasia in humans and hypoplasia of endochondral bones in mice (9, 34). This phenotype has also been produced by stabilization of β-catenin in chondrocytes (12).

These experiments demonstrate that mutations in *MAP3K1* caused abnormal testicular development by downregulating SOX9 expression mediated by RHOA and by the β-catenin negative feedback loop. Furthermore, the mutated MAP3K1

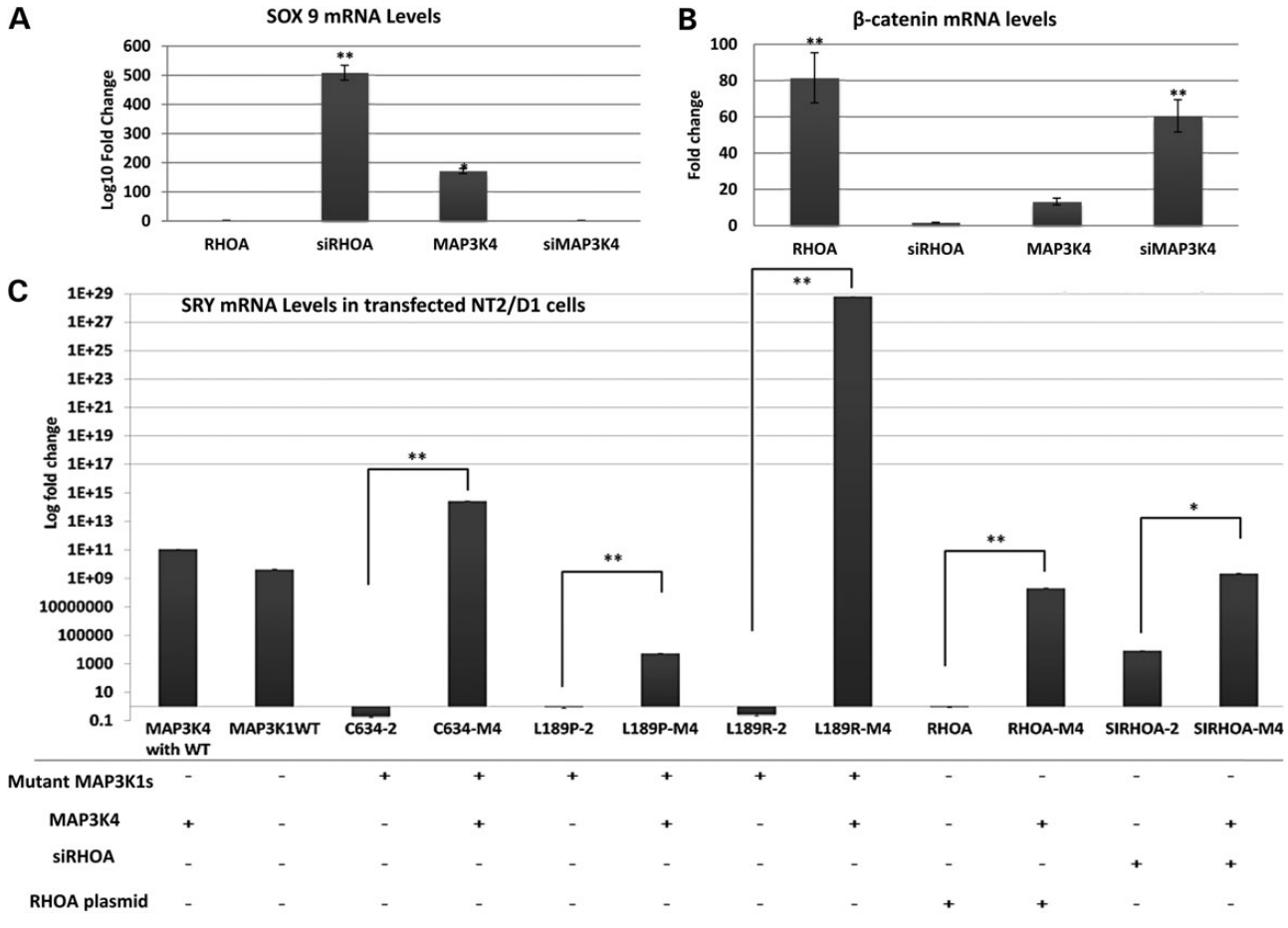

Figure 6. Over and under expression of MAP3K4 or RHOA modulates SOX9 and β-catenin mRNA expression levels. Taqman qPCR analysis performed after 24 h for all transfected NT2/D1 cells with *MAP3K4* or *RHOA* expression plasmids and/or siRNA to *RHOA* or *MAP3K4*. All results were normalized to housekeeping gene, GAPDH, and compared with control NT2/D1 cells transfected with empty plasmids by Student's *t*-test, $^{*}P < 0.05$ and $^{**}P < 0.005$. (**A**) Quantification of normalized SOX9 mRNA expression (*Y*-axis is fold change relative to transfected cells with empty plasmids) and compared in a pairwise fashion (overexpression versus siRNA). The expression of SOX9 was increased by RHOA inhibition and MAP3K4 overexpression and marked decrease when NT2/D1 cells were transfected with RHOA cDNA or MAP3K4 siRNA mRNA. (**B**) Quantification of normalized β-catenin expression (*Y*-axis is fold change relative to transfected cells with empty plasmids) and compared in a pairwise fashion (overexpression versus siRNA). The expression of β-catenin was increased when NT2/D1 cells were transfected with RHOA cDNA or MAP3K4 siRNA. Conversely, cells transfected with RHOA siRNA or MAP3K4 cDNA showed dramatic decrease of β-catenin expression. (**C**) Transfection of wild-type or mutant MAP3K1 or MAP3K4 cDNAs modulate SRY mRNA expression levels. qPCR analysis of mRNA at 24 h after in NT2/D1 cells co-transfected with MAP3K1 or mutant MAP3K1s with MAP3K4 and RHOA or siRNA to RHOA with MAP3K4 expression plasmids. For the qPCR experiments, the results were normalized to the housekeeping gene, GAPDH, and compared with control NT2/D1 cells transfected with empty plasmids by Student's *t*-test, $P < 0.001$ and $^{**}P < 0.0001$. Bar graph quantification of normalized SRY mRNA expression levels (*Y*-axis is fold change relative quantity to empty plasmids). The expression of SRY mRNA was markedly decreased when transfected with mutant MAP3K1cDNAs. Cells transfected with wild-type MAP3K1 cDNAs and cotransfected with MAP3K4 showed dramatic increases in SRY expression. The greatest reduction of SRY was observed for mutant c.634-8A transfected cells (77%), followed by p.L189P (65%), and for p.L189R (52%). When MAP3K4 was co-transfected in a separate rescue experiments, SRY mRNA levels were restored compared with mutant only transfections. Expression of SRY increased above wild-type levels in mutant C634-8A and L189R co-transfected with MAP3K4.When MAP3K4 was co-transfected with RHOA, the effect on SRY expression was normalized to wild-type levels. Similarly, a restorative increase of SRY expression was observed when MAP3K4 was co-transfected with siRNA to RHOA.

proteins upregulated β-catenin expression and activity through increased phosphorylation of p38 and ERK1/2 and increased binding of AXIN1 and FRAT1 proteins. Seemingly, a threshold of cofactor binding and kinase activity must be exceeded to affect gonadal development. The p.K246E mutation reported here increased p38 kinase activity at modest level, yet had no effect on RHOA binding, ERK1/2 phosphorylation, nor testicular development. This mutation is representative of a series of 23 rare missense variants in the *MAP3K1* gene that have been reported in dbSNP, each with an individual allele frequency <1% and collectively with an allele frequency of 1.56% (http://www.ncbi.nlm.nih.gov/projects/SNP/snp_ref.cgi?locusId=4214). Some of these may alter the cofactor binding and kinase activity above the threshold in aggregate to cause abnormal testicular development and explain the seeming prevalence of *MAP3K1* mutations that we have observed as a cause for 46,XY gonadal dysgenesis (15).

MATERIALS AND METHODS

Cell culture

This study was approved by the institutional review boards of Albert Einstein College of Medicine and the collaboration

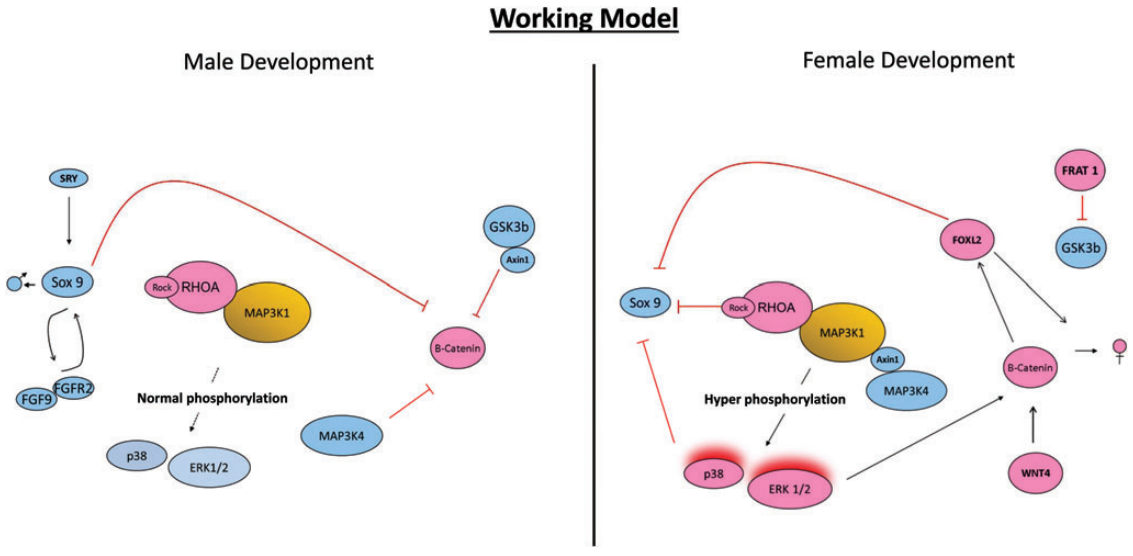

Figure 7. Role of MAP3K1 cofactors and downstream targets in promoting gonadal determination. Testis-promoting factors are shown in blue and ovary-promoting factors are shown in red. Factors that promote the action of a downstream target are shown as arrows. Factors that block the action of a downstream target are shown as red lines ending in bars. Male development: SRY, RAC1 (data not shown), MAP3K4 and AXIN1 all promote the expression of SOX9 and, through a feedforward loop, FGF9. SOX9, AXIN1 and GSK3β promote the destabilization of β-catenin and, thus, create a block to ovarian development. Female development: RHOA, phosphorylated p38 and ERK1/2 and FOXL2 downregulate the expression of SOX9 and, thus, the resulting feedforward loop and block to ovarian development. Phosphorylated p38 and ERK1/2 and AXIN1 (via destabilized GSK3β) and FRAT1 promote the stabilization of β-catenin and the upregulation of the downstream targets, FOXL2 and FST. Possible sequestration of AXIN1 and MAP3K4 onto mutant MAP3K1 enhances β-catenin stabilization. Gain-of-function mutations in the MAP3K1 gene mimic the ovarian determining pathway, overriding the testis-determining signal from an expressed, wild-type SRY gene.

with University of Pavia and appropriate informed consent was obtained from all human subjects. Isolated and EBV immortalized B-LCLs, and human Neuron-committed Teratocarcinoma (NT2/D1) cells, were maintained in RPMI 1640 and DMEM (Life Technologies, Grand Island, NY, USA) supplemented with 10 and 15% fetal bovine serum, respectively, and cultured in CO_2 jacketed 37°C incubators according to the manufacturer's recommendations (GIBCO, Life Technologies). The NT2/D1 cells were starved for 24 h for cell synchronization prior to all transfection experiments.

Co-immunoprecipitation western blots and FVA

At 85% confluence, NT2/D1 cells were washed and collected with cold phosphate buffered saline (PBS) and then lysed in cold lysis buffer, containing 150 mM NaCl, 30 mM Tris (pH 7.5), 1 mM EDTA, 1% Triton X-100, 10% glycerol, 0.1 mM PMSF, 0.5 mM DTT and protease and phosphatase inhibitor cocktail tablets (EDTA-free) (Roche Applied Science, Mannheim, Germany). FVA was performed as previously described with the following modifications (16). After centrifugation (12 000*g* for 30 min at 48°C), the cellular lysates were precleared with IgG-Dynabeads (Life Technologies) for at least 4 h at 4°C. Immunoprecipitation of endogenous complexes were carried out by incubating the cellular lysates with anti-MAP3K1 antibody-conjugated, epoxy-coated Dynabeads or mouse IgG immobilized on Protein G Dynabeads (Life Technologies) at 4°C overnight. Immunocomplexes were washed with cold flow cytometry buffer three times and resuspended in 50 µl of the flow cytometry buffer, containing Tris, pH 7.4, 50 mM, sodium azide 0.02%, defined grade fetal bovine serum 5%, PBS, pH 7.4. The immunoprecipitated beads were sorted and analyzed on BDFacsCanto II flow cytometer (BD Biosciences, San Jose, CA, USA) followed by concurrent western blot analysis of 500 000 beads remained after FVA. The beads were boiled in western loading buffer with SDS at 95°C for 10 min prior to western gel loading. Gradient Bis–Tris 4–12% gels were used (Life Technologies), and transferred using iBlot and the transfer kit for 8 min followed by BSA blocking, containing BSA 1%, host serum 1%, sodium azide 0.02%, PBS, pH 7.4, 2.7 mM KCl. The blots were hybridized overnight on a rocker in 4°C by using anti-MAP3K1 (clone C-22, Santa Cruz, CA, USA), MAP3K4 (clone 4D3, Santa Cruz, CA, USA), GSK3β (clone 27C10, Cell Signalling Inc., Danvers, MA, USA), RHOA (Ser1490, Cell Signaling), AXIN1 (Abcam, Cambridge, UK), β-catenin (clone B-5-1-2, Sigma-Aldrich, St. Louis, MO, USA) and SOX9 (Abcam, Cambridge, UK) antibodies, as described.

cDNA and RNA interference constructs

A full-length *MAP3K1* wild-type plasmid driven by a CMV promoter was used as a template for mutagenesis PCR for the three mutations studied, as described below. *RHOA* and *MAP3K4* Origene True ORF plasmids (Origene, Rockville, MD, USA) were used to transfect NT2/D1 cells, including those that were performed to demonstrate specificity of targeted knockdown by siRNAs. Predesigned Stealth siRNA triplex targeting transcripts of the human *RHOA* and *MAP3K4* (Life Technologies) were used to knockdown RHOA or MAP3K4 in NT2/D1 cells. Off-target scrambled control siRNA pool was used as a control (Life Technologies). Fifteen millimolal siRNA was delivered

into 1×10^5 NT2/D1 cells using the Lipofectamine transfection reagents (Life Technologies). Gene expression of the mRNA and protein were examined 48 h after transfection by qPCR, western blot and DCW analysis. For DCW, 1×10^6 cells were counted for each sample and 16% formaldehyde was added directly into the culture medium to a final concentration of 1.5%). The cells were incubated for 10 min at 25°C or room temperature, then pelleted by low-speed centrifugation at 2000 *g* at 4°C. The cell pellet was resuspended by vortexing in 500 μl ice-cold methanol and incubated on ice for 5 min. Cells were stored at −80°C with minimum degradation. Prior to DCW analysis, 50–100 μL of cells or ∼500 million cells were stained with fluorescently labeled antibodies at 1:100.

Reporter gene assays and transient transfection

The TCF/LEF Cignal luciferase reporter assay is a pre-formulated mix of Renilla with a transfection-ready TCF/LEF reporter construct, negative control or positive control (Qiagen, Valencia, CA, USA). The transcription factor reporters and controls were transfected in parallel with identical experimental parameters. Dual-luciferase results were calculated for each transfectant by normalizing to internal fluorescence of Renilla and then calculating the change in the activity by comparing the normalized luciferase activities of the reporter in treated versus untreated transfectants. The identically treated negative control transfectants served as specificity controls. Transfection efficiency was determined from the activity of green fluorescent protein positive control as well as a positive control for both the firefly and Renilla luciferase assays. The cells were lysed after 24 and 48 h using luciferase lysis buffer (Promega Corp., Madison, WI, USA), and luciferase activities were measured using the dual-luciferase reporter assay system on dual injector Biotek Synergy H1 reader (Biotek, Winooski, VT, USA). All transfection experiments were performed in triplicates.

In the siRNA knockdown co-transfection experiments, NT2/D1 cells were seeded at a density of 1×10^5 cells/6-well plate in triplicates and siRNA targeting the human *RHOA* or *MAP3K4* gene or control non-targeting medium GC content siRNA was delivered to NT2/D1 cells the following day after overnight serum deprivation in DMEM-only media. After 24 h, cells were transfected with Cignal TCF/LEF luciferase reporter mix constructs according to manufacturer's protocol using Lipofectamine 2000 (Life Technologies).

In shRNA knockdown co-transfection experiments using luciferase assays to examine the effect of wild-type *MAP3K1* and point mutations in *MAP3K1*, NT2/D1 cells were plated in 40–50% density in 24-well plates and 2.5 ng/well *MAP3K1* constructs or control DNA were transfected together with reporter plasmid and internal control plasmid several hours after seeding.

Quantitative RT–PCR

Quantitative RT–PCR (qRT–PCR) experiments were analyzed in a VIAA7 real-time PCR detection system (Life Technologies) using Taqman gene expression master mix (Life Technologies). Values were normalized using β-actin as a control. The following Taqman assays were used for examining the effect of *MAP3K1*, *RHOA* and *MAP3K4* after transfections:

Taqman gene expression assay ID	Target gene
HS00394890	*MAP3K1*
HS00245958	*MAP3K4*
KS00165814	*SOX9*
HS01552926	*FGFR2*
HS00181829	*FGF9*
HS00355049	*CTNNB1* (β-catenin)
HS00357608	*RHOA*
HS99999903	*ACTB*
HS00846401	*FOXL2*
Hs00976796	*SRY*

Site-directed mutagenesis-*MAP3K1* mutants were generated using the Quick Change Site-Directed Mutagenesis II kit (Stratagene, Cedar Creek, TX, USA). Wild-type full-length *MAP3K1* expression vector (a kind gift from Dr. Michael Karin) was used as a template for PCR based mutagenesis with primer arms flanking 22 bases on each side of the mutation site.

Data analysis

Comparison of differences between Cignal luciferase activity assay and qRT–PCR expression was performed using the two-tailed Student's *t*-test (where equal variance between groups was assumed). A *P*-value of <0.05 was considered statistically significant.

SUPPLEMENTARY MATERIAL

Supplementary Material is available at *HMG* online.

ACKNOWLEDGEMENTS

The authors thank Lydia Tesfa for technical assistance with the FVA assays, Jacklyn Lee and Benjamin Metrikin for technical assistance with the transfection experiments and Stephanie Boisson-Dupuis and Jean-Laurent Casanova for the K246E cell line.

Conflict of Interest statement. None declared.

REFERENCES

1. Cool, J. and Capel, B. (2009) Mixed signals: development of the testis. *Semin. Reprod. Med.*, **27**, 5–13.
2. Wilhelm, D. and Koopman, P. (2006) The makings of maleness: towards an integrated view of male sexual development. *Nat. Rev. Genet.*, **7**, 620–631.
3. Eggers, S. and Sinclair, A. (2012) Mammalian sex determination-insights from humans and mice. *Chromosome Res.*, **20**, 215–238.
4. Sinclair, A.H., Berta, P., Palmer, M.S., Hawkins, J.R., Griffiths, B.L., Smith, M.J., Foster, J.W., Frischauf, A.M., Lovell-Badge, R. and Goodfellow, P.N. (1990) A gene from the human sex-determining region encodes a protein with homology to a conserved DNA-binding motif. *Nature*, **346**, 240–244.
5. Parma, P., Radi, O., Vidal, V., Chaboissier, M.C., Dellambra, E., Valentini, S., Guerra, L., Schedl, A. and Camerino, G. (2006) R-spondin1 is essential in sex determination, skin differentiation and malignancy. *Nat. Genet.*, **38**, 1304–1309.
6. Koopman, P., Gubbay, J., Vivian, N., Goodfellow, P. and Lovell-Badge, R. (1991) Male development of chromosomally female mice transgenic for Sry. *Nature*, **351**, 117–121.

7. Vidal, V.P., Chaboissier, M.C., de Rooij, D.G. and Schedl, A. (2001) Sox9 induces testis development in XX transgenic mice. *Nat. Genet.*, **28**, 216–217.
8. Berta, P., Hawkins, J.R., Sinclair, A.H., Taylor, A., Griffiths, B.L., Goodfellow, P.N. and Fellous, M. (1990) Genetic evidence equating SRY and the testis-determining factor. *Nature*, **348**, 448–450.
9. Foster, J.W., Dominguez-Steglich, M.A., Guioli, S., Kwok, C., Weller, P.A., Stevanovic, M., Weissenbach, J., Mansour, S., Young, I.D., Goodfellow, P.N. *et al.* (1994) Campomelic dysplasia and autosomal sex reversal caused by mutations in an SRY-related gene. *Nature*, **372**, 525–530.
10. Jordan, B.K., Mohammed, M., Ching, S.T., Delot, E., Chen, X.N., Dewing, P., Swain, A., Rao, P.N., Elejalde, B.R. and Vilain, E. (2001) Up-regulation of wnt-4 signaling and dosage-sensitive sex reversal in humans. *Am. J. Hum. Genet.*, **68**, 1102–1109.
11. Maatouk, D.M., DiNapoli, L., Alvers, A., Parker, K.L., Taketo, M.M. and Capel, B. (2008) Stabilization of beta-catenin in XY gonads causes male-to-female sex-reversal. *Hum. Mol. Genet.*, **17**, 2949–2955.
12. Akiyama, H., Lyons, J.P., Mori-Akiyama, Y., Yang, X., Zhang, R., Zhang, Z., Deng, J.M., Taketo, M.M., Nakamura, T., Behringer, R.R. *et al.* (2004) Interactions between Sox9 and beta-catenin control chondrocyte differentiation. *Genes Dev.*, **18**, 1072–1087.
13. Murakami, S., Kan, M., McKeehan, W.L. and de Crombrugghe, B. (2000) Up-regulation of the chondrogenic Sox9 gene by fibroblast growth factors is mediated by the mitogen-activated protein kinase pathway. *Proc. Natl. Acad. Sci. USA*, **97**, 1113–1118.
14. Woods, A., Wang, G. and Beier, F. (2005) Rhoa/ROCK signaling regulates Sox9 expression and actin organization during chondrogenesis. *J. Biol. Chem.*, **280**, 11626–11634.
15. Pearlman, A., Loke, J., Le Caignec, C., White, S., Chin, L., Friedman, A., Warr, N., Willan, J., Brauer, D., Farmer, C. *et al.* (2010) Mutations in MAP3K1 cause 46,XY disorders of sex development and implicate a common signal transduction pathway in human testis determination. *Am. J. Hum. Genet.*, **87**, 898–904.
16. Loke, J. and Ostrer, H. (2012) Rapidly screening variants of uncertain significance in the MAP3K1 gene for phenotypic effects. *Clin. Genet.*, **81**, 272–277.
17. Warr, N., Bogani, D., Siggers, P., Brixey, R., Tateossian, H., Dopplapudi, A., Wells, S., Cheeseman, M., Xia, Y., Ostrer, H. *et al.* (2011) Minor abnormalities of testis development in mice lacking the gene encoding the MAPK signalling component, MAP3K1. *PLoS ONE*, **6**, e19572.
18. Sue Ng, S., Mahmoudi, T., Li, V.S., Hatzis, P., Boersema, P.J., Mohammed, S., Heck, A.J. and Clevers, H. (2010) MAP3K1 functionally interacts with Axin1 in the canonical Wnt signalling pathway. *Biol. Chem.*, **391**, 171–180.
19. Fraser, E., Young, N., Dajani, R., Franca-Koh, J., Ryves, J., Williams, R.S., Yeo, M., Webster, M.T., Richardson, C., Smalley, M.J. *et al.* (2002) Identification of the axin and frat binding region of glycogen synthase kinase-3. *J. Biol. Chem.*, **277**, 2176–2185.
20. Nakamura, T., Hamada, F., Ishidate, T., Anai, K., Kawahara, K., Toyoshima, K. and Akiyama, T. (1998) Axin, an inhibitor of the Wnt signalling pathway, interacts with beta-catenin, GSK-3beta and APC and reduces the beta-catenin level. *Genes Cells*, **3**, 395–403.
21. Knower, K.C., Sim, H., McClive, P.J., Bowles, J., Koopman, P., Sinclair, A.H. and Harley, V.R. (2007) Characterisation of urogenital ridge gene expression in the human embryonal carcinoma cell line NT2/D1. *Sex. Dev.*, **1**, 114–126.
22. Bernard, P., Ryan, J., Sim, H., Czech, D.P., Sinclair, A.H., Koopman, P. and Harley, V.R. (2012) Wnt signaling in ovarian development inhibits Sf1 activation of Sox9 via the Tesco enhancer. *Endocrinology*, **153**, 901–912.
23. Topol, L., Chen, W., Song, H., Day, T.F. and Yang, Y. (2009) Sox9 inhibits Wnt signaling by promoting beta-catenin phosphorylation in the nucleus. *J. Biol. Chem.*, **284**, 3323–3333.
24. Knower, K.C., Kelly, S., Ludbrook, L.M., Bagheri-Fam, S., Sim, H., Bernard, P., Sekido, R., Lovell-Badge, R. and Harley, V.R. (2011) Failure of SOX9 regulation in 46XY disorders of sex development with SRY, SOX9 and SF1 mutations. *PLoS ONE*, **6**, e17751.
25. Ding, Q., Xia, W., Liu, J.C., Yang, J.Y., Lee, D.F., Xia, J., Bartholomeusz, G., Li, Y., Pan, Y., Li, Z. *et al.* (2005) Erk associates with and primes GSK-3beta for its inactivation resulting in upregulation of beta-catenin. *Mol. Cell.*, **19**, 159–170.
26. Thornton, T.M., Pedraza-Alva, G., Deng, B., Wood, C.D., Aronshtam, A., Clements, J.L., Sabio, G., Davis, R.J., Matthews, D.E., Doble, B. *et al.* (2008) Phosphorylation by p38 MAPK as an alternative pathway for GSK3beta inactivation. *Science*, **320**, 667–670.
27. Bikkavilli, R.K. and Malbon, C.C. (2009) Mitogen-activated protein kinases and Wnt/beta-catenin signaling: molecular conversations among signaling pathways. *Commun. Integr. Biol.*, **2**, 46–49.
28. Gallagher, E.D., Gutowski, S., Sternweis, P.C. and Cobb, M.H. (2004) Rhoa binds to the amino terminus of MEKK1 and regulates its kinase activity. *J. Biol. Chem.*, **279**, 1872–1877.
29. Tew, S.R. and Hardingham, T.E. (2006) Regulation of SOX9 mRNA in human articular chondrocytes involving p38 MAPK activation and mRNA stabilization. *J. Biol. Chem.*, **281**, 39471–39479.
30. Kumar, D. and Lassar, A.B. (2009) The transcriptional activity of Sox9 in chondrocytes is regulated by RhoA signaling and actin polymerization. *Mol. Cell. Biol.*, **29**, 4262–4273.
31. Luo, W., Ng, W.W., Jin, L.H., Ye, Z., Han, J. and Lin, S.C. (2003) Axin utilizes distinct regions for competitive MEKK1 and MEKK4 binding and JNK activation. *J. Biol. Chem.*, **278**, 37451–37458.
32. Ostrer, H. (2011) Changing the game with whole exome sequencing. *Clin. Genet.*, **80**, 101–103.
33. Bogani, D., Siggers, P., Brixey, R., Warr, N., Beddow, S., Edwards, J., Williams, D., Wilhelm, D., Koopman, P., Flavell, R.A. *et al.* (2009) Loss of mitogen-activated protein kinase kinase kinase 4 (MAP3K4) reveals a requirement for MAPK signalling in mouse sex determination. *PLoS Biol.*, **7**, e1000196.
34. Wagner, T., Wirth, J., Meyer, J., Zabel, B., Held, M., Zimmer, J., Pasantes, J., Bricarelli, F.D., Keutel, J., Hustert, E. *et al.* (1994) Autosomal sex reversal and campomelic dysplasia are caused by mutations in and around the SRY-related gene SOX9. *Cell*, **79**, 1111–1120.